

AD-A245 848

Final scientific report
AFOSR 90-0357

(2)

"Intrinsic stress in reactively magnetron
sputtered metal-nitride/oxide films."

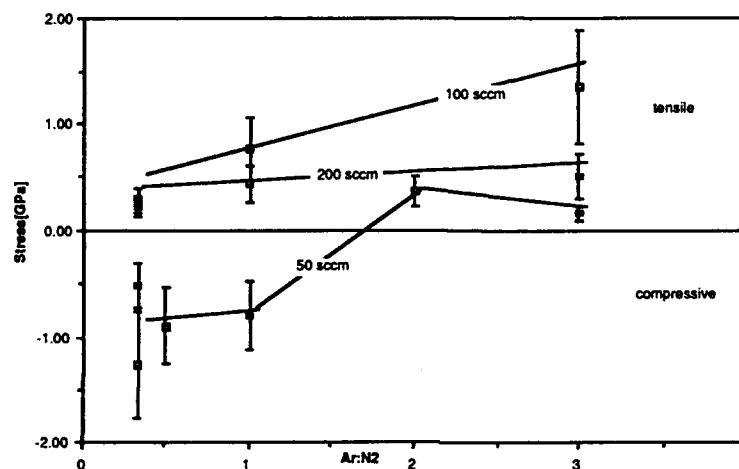


Fig.9.: Measured stress values of reactively dc magnetron sputtered AlN films for total gas flows of 50sccm, 100sccm, and 200sccm at different sputtering gas compositions (Ar to N₂ ratio).

Principal investigator: Prof. Dr. phil. H. K. Pulker

DTIC
ELECTE
FEB 10 1992
S D

E. Rille
R. Zarwasch
H. Öfner

Universität Innsbruck
Institut für Experimentalphysik
Technikerstraße 15
A-6020 Innsbruck
Austria

This document has been approved
for public release and its
distribution is unlimited.



DEPARTMENT OF THE AIR FORCE
AIR FORCE OFFICE OF SCIENTIFIC RESEARCH (AFSC)
EUROPEAN OFFICE OF AEROSPACE RESEARCH AND DEVELOPMENT
BOX 14, FPO NEW YORK 09510-0200
Autovon Tel: 235-4474
Telefax: 44-71-402-9618

24 January 1992

REPLY TO
ATTN OF: **LRE**

SUBJECT: **EOARD-TR-, Final Scientific Report, "Intrinsic Stress in Reactively Magnetron Sputtered Metal-Nitride/Oxide Films"**

TO: **DTIC/Air Force Liaison Representative**
Cameron Station
Alexandria, VA 22304-6145

1. I certify that the subject TR has been reviewed by EOARD and approved for public release in accordance with AFR 80-45/AFSC Sup 1. It may be made available or sold to the general public and foreign nationals.
2. Distribution statement "A" appears on the subject TR and the Standard Form 298 as required by AFRs 80-44 and 80-45.

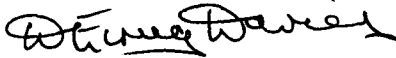
D. EIRUG DAVIES, Ph.D.
Chief, Semiconductors/S.S. Physics

- 2 Atch
1. EOARD-TR- (2cys)
2. DTIC Form 50

EOARD TR 92-02

This report has been reviewed and is releasable to the National Technical Information Service (NTIS).
At NTIS it will be releasable to the general public, including foreign nations.

This technical report has been reviewed and is approved for publication.



D. EIRUG DAVIES, Ph.D.
Chief, Semiconductors/S.S. Physics



RONALD J. LISOWSKI, Lt Col, USAF
Chief Scientist

98 2 07 010

92-03164
■■■■■■■■

REPORT DOCUMENTATION PAGE			OMB No. 0704-0188
<small>Public reporting burden for this collection of information is estimated to average 1 hour per response, including the time for reviewing instructions, searching existing data sources, gathering and maintaining the data needed, and completing and reviewing the collection of information. Send comments regarding this burden estimate or any other aspect of this collection of information, including suggestions for reducing the burden, to Washington Headquarters Services, Directorate for Information Operations and Reports, 1215 Jefferson Davis Highway, Suite 1204, Arlington, VA 22202-4302, and to the Office of Management and Budget, Paperwork Reduction Project (0704-0188), Washington, DC 20503.</small>			
1. AGENCY USE ONLY (Leave blank)	2. REPORT DATE	3. REPORT TYPE AND DATES COVERED Final Technical Report 1/9/90-31/8/91	
4. TITLE AND SUBTITLE "Intrinsic Stress in Reactively Magnetron Sputtered Metal-Nitride/Oxide Films"		5. FUNDING NUMBERS G AFOSR-90-0357	
6. AUTHOR(S) H.K. PULKER & E. RILLE			
7. PERFORMING ORGANIZATION NAME(S) AND ADDRESS(ES) University of Innsbruck Institut für Experimentalphysik Technikerstraße 25 A-6020 Innsbruck, Austria		8. PERFORMING ORGANIZATION REPORT NUMBER	
9. SPONSORING/MONITORING AGENCY NAME(S) AND ADDRESS(ES) Sponsoring Agency: Weapons Laboratory Kirtland AFB, NM 87117-6008 Sponsoring/Monitoring Agency: European Office of Aerospace Research and Development, Box 14 FBO New York 09510-0200		10. SPONSORING/MONITORING AGENCY REPORT NUMBER EOARD TR 92-02	
11. SUPPLEMENTARY NOTES			
12a. DISTRIBUTION/AVAILABILITY STATEMENT Approved for public release; Distribution unlimited		12b. DISTRIBUTION CODE	
13. ABSTRACT (Maximum 200 words) The reactive dc magnetron sputtering of AlN films and the in-situ stress measurements were performed in a 0.45m ³ cylindrical vacuum chamber, which was typically pumped down to 2x10 ⁻⁴ Pa by an oil diffusion pump. The stress was determined by the beam bending method. Structural details were revealed by transmission electron microscopy (TEM) and high energy (80keV) electron beam diffraction (EBD). Our own preliminary measurements enabled the choice of a promising range of variation for the parameters Ar/N ₂ -ratio and total gas flow. The argon to nitrogen ratios varied from 1:3 to 3:1 at three different total gas flows: 50sccm, 100sccm, and 200sccm. A polycrystalline hexagonal structure of all the AlN films was found by electron beam diffraction. In the case of low sputtering gas pressure of about 2x10 ⁻¹ Pa a preferential orientation with the crystallographic c-axis orthogonal to the substrate was observed. This preferential orientation (texture) vanished as the sputtering gas pressure reached about 8x10 ⁻¹ Pa. The refractive index at a wavelength of 550nm of the 50sccm series scattered around 2.12, for the 100sccm samples the mean value is 2.05, and for the 200sccm samples a mean value of 1.97 was found. The AlN films prepared at gas flows of 100sccm and 200sccm showed only tensile stresses (up to 1GPa). The 50sccm series showed a transition from compressive (-1.3GPa) to tensile film stresses (0.3GPa) when the Ar/N ₂ ratio was increased to more than 2:1. In this flow regime stress tuning was therefore possible.			
14. SUBJECT TERMS REACTIVE DC MAGNETRON SPUTTERING, INTRINSIC STRESS		15. NUMBER OF PAGES 36	
		16. PRICE CODE	
17. SECURITY CLASSIFICATION OF REPORT Unclassified	18. SECURITY CLASSIFICATION OF THIS PAGE Unclassified	19. SECURITY CLASSIFICATION OF ABSTRACT Unclassified	20. LIMITATION OF ABSTRACT

Summary

The reactive dc magnetron sputtering of AlN films and the in-situ stress measurements were performed in a 0.45m^3 cylindrical vacuum chamber, which was typically pumped down to $2 \times 10^{-4}\text{Pa}$ by an oil diffusion pump before backfilling with the sputtering gases.

The stress was determined by the beam bending method.

A Perkin-Elmer 330 Photospectrometer was used to measure the optical transmittance of the various AlN samples. The wavelength range under investigation was 185nm to 850nm. Transmission data were used to calculate the refractive index of AlN films .

Structural details were revealed by transmission electron microscopy (TEM) and high energy (80keV) electron beam diffraction (EBD). Films for these investigations were deposited onto very thin (5-10nm) amorphous carbon supports.

Our own preliminary measurements enabled the choice of a promising range of variation for the parameters Ar/N₂-ratio and total gas flow. The argon to nitrogen ratios varied from 1:3 to 3:1 at three different total gas flows: 50sccm, 100sccm, and 200sccm.

According to our AES measurements and the accuracy of this method all films were composed of at least 95% AlN (with small amounts of oxygen).

A polycrystalline hexagonal structure of all the AlN film was found by electron beam diffraction. In the case of low sputtering gas pressure of about $2 \times 10^{-1}\text{Pa}$ a preferential orientation with the cristallographic c-axis orthogonal to the substrate was observed. This preferential orientation (texture) vanished as the sputtering gas pressure reached about $8 \times 10^{-1}\text{Pa}$.

The refractive index at a wavelength of 550nm of the 50sccm series scattered around 2.12, for the 100sccm samples the mean value is 2.05, and for the 200sccm samples a mean value of 1.97 was found.

Similar to rf sputter-deposited AlN films our reactive dc magnetron sputtered AlN films revealed also three regions in the short wave absorption edge. AlN film samples prepared at a total gas flow of 200sccm had inverse slope values between 1.01eV to 1.05eV. Films deposited at 100sccm and 50sccm gave inverse slope values from 1.13eV to 1.24eV and from 1.19eV to 1.29eV respectively.

The AlN films prepared at gas flows of 100sccm and 200sccm showed only tensile stresses (up to 1GPa). The 50sccm series showed a transition from compressive (-1.3GPa) to tensile film stresses (0.3GPa) when the Ar/N₂ ratio was increased to more than 2:1. In this flow regime stress tuning was therefore possible.

Although the extreme values of the stress in AlN films were -0.9GPa on the compressive and +1.2GPa on the tensile side, no significant differences in the chemical composition could be detected. This result supports the knowledge that predominantly the film microstructure determines the intrinsic stress.

Contents

1. Introduction
2. Methods
 - 2.1 Experimental Apparatus
 - 2.2 Process Conditioning
3. Results
 - 3.1 Plasma parameters
 - 3.1.1 Kinetic temperature for pure Al sputtering
 - 3.1.2 Plasma-potential and floating-potential for AlN reactive dc magnetron-sputtering
 - 3.2 Thin film parameters
 - 3.2.1 Substrate temperature
 - 3.2.2 Deposition rates
 - 3.2.3 Chemical Composition
 - 3.2.4 Morphology and structure
 - 3.2.5 Optical data
 - 3.3 Stress
 - 3.3.1 Stress tuning
 - 3.3.2 Reactive Sputtering Model
4. Conclusions
 - 4.1 Deposition parameters
 - 4.2 Morphology and structure
 - 4.3 Optical absorption
 - 4.4 Thin Film Stress
 - 4.4.1 Model
 - 4.4.2 Reactive dc magnetron sputtering
5. References

Accession For	
NTIS CRASI	<input checked="" type="checkbox"/>
DTIC TAB	<input type="checkbox"/>
Unannounced	<input type="checkbox"/>
Justification	
By	
Distribution /	
Availability Codes	
Dist	Avail. and/or Special
A-1	



1. Introduction

Thin films deposited by physical vapor deposition (PVD) processes are generally in a state of mechanical stress, which can be regarded assumptionally as the sum of an external, a thermal, and an intrinsic component. The external component can be neglected but a thermal component has to be considered, because of thermal input energies during film formation and possible differences in expansion between substrate and film material. The intrinsic component is understood to be the remaining structure sensitive part of the film stress. Therefore the intrinsic mechanical stress represents a characteristic property of a film. Unpleasant macroscopic effects such as blisters in the case of compressive stress or cracks in the tensile case appear if the magnitude of the film stress exceeds either the adhesive force between film and substrate and/or the cohesive forces between film forming crystallites.^{1, 2}

The deposition of AlN by reactive dc magnetron sputtering allows for tuning of the arising intrinsic stress by the variation of certain process parameters³⁻⁹, within condition for proper film stoichiometry.

For practical use of the stress tuning it is important to know to what extent stress can be influenced. So the application sets the limits to the minimum or maximum stress that the coating, fulfilling the specifications, can be tuned to.

In reactive sputtering the desired product is created by chemical reactions of components of the sputtering gas with sputtered metal atoms from the cathode. As this reaction also leads to a partial coverage of the cathode with reactive products hysteresis in the dependence of reactive gas partial pressure on

reactive gas flow is observed. To the reactive sputtering model¹⁰ describing these hysteresis processes an energy dependent sputtering yield was introduced.

The connected optical and structural properties were also studied.

2. Methods

2.1 Experimental Apparatus

2.1.1 Vacuum

The production of the AlN films and the in-situ stress measurements were performed using a 0.45m³ vacuum chamber, which was typically pumped down to 2x10⁻⁴Pa by an oil diffusion pump before letting the sputtering gases inside.

As a sputtering source a planar magnetron cathode (PM) of the type Balzers EK 510 was used (see fig 1). The PM consisted of an aluminum target (99.999% purity; 12.5x25cm² area) and was mounted in an upright position. The power supply for the PM was a Balzers MPS 105 with a maximum power output of 5kW. The power supply could be run in two different modes. During all measurements the MPS ran in the power controlled mode, which kept discharge current times discharge voltage constant at 1kW.

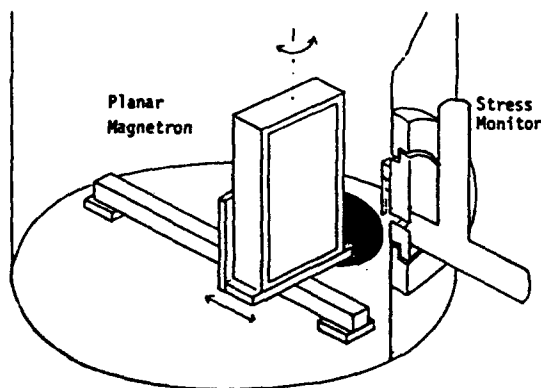


Fig. 1.: Magnetron and stress monitor setup.

Argon and nitrogen entered the chamber separately, controlled by mass flow controllers.

Discharge voltages between 250V and 300V resulted as a consequence of constant power mode, different total gas flows (50-200sccm) and Ar/N₂ ratios (3:1, 1:1, 1:3).

To avoid thermal effects due to a high thermal expansion coefficient of the substrate only fused silica longish substrates were used.

2.1.2 Stress monitor

For determining the stress we used the bending beam method. That is, the stress occurring in the film is transmitted to the substrate, causing it to deform. The deformation can be measured directly, or the compensating force required to offset the strain can be determined. The first approach was selected in the work reported here; the substrate deformation was measured optically. Fig 2 shows the monitor schematically. If reproducible results are to be obtained by this indirect method, the film material must show adequate adhesion to the substrate. Meaningful conclusions from the measured values are possible only when no stress relaxing cracks or blisters have yet formed in the film.

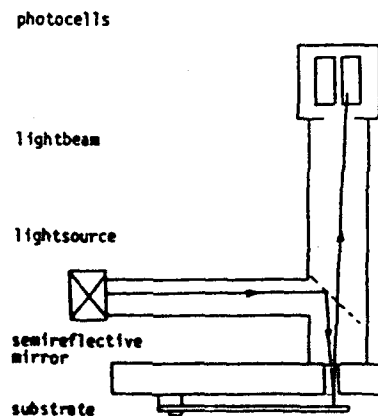


Fig. 2.: Stress monitor

The substrate in each trial was a glass plate clamped at one end and having the following dimensions: length 80mm, width 10mm, thickness 0.7-1.5mm.

Intrinsic stresses arising in the film manifest themselves by shrinking (tensile stress) or expanding (compressive stress) the film in the film plane. If the adhesion between film and substrate is sufficiently high, these forces cause the system to deform, as already mentioned: for a glass plate clamped at one end the deformation appears as a deflection of the free end. This deflection, of the orders of micrometers, is detected by a light spot reflected from the surface of the free end, which is optically magnified and imaged in a photoelectric detection system. The detector essentially consists of two photocells. The difference between the photocell currents yields an analog signal, which is plotted continuously throughout the film deposition process.

The stress values of the film were obtained by comparing the measurements with calibration measurements performed before film deposition. For calibration, the deflection was produced by loading the free end of the glass plate in steps, with precisely known platinum weights. The sensitivity of the stress monitor is in the range of a few percent of the magnitude of the measured stress.

The in-situ stress monitor was flanged on to the chamber wall. The surface of the substrate of the monitor was parallel to the target and centred in respect to the target area. The target to substrate distance was kept at 0.14m.

2.1.3 Thin film evaluation

A Perkin-Elmer 330 Photospectrometer was used to measure the light transmission of the various AlN samples. The wavelength range under investigation was 185nm to 850nm. From the transmission data the refractive index of AlN films was calculated.

Applying the evaluation method of Swanepoel¹¹, just one single transmission spectrum in the range between 3eV and 6.2eV had to be sampled to obtain the absorption data of each film.

Structural details of the films were revealed by transmission electron microscopy (TEM) and high energy (80keV) electron beam diffraction (EBD). Films for these investigations were deposited onto very thin (5-10nm) amorphous carbon films.

2.2 Process Conditioning

The presence of a high voltage gas discharge and dielectric thin films on supporting structures caused some difficulties in reaching a satisfying reproducibility of the film stress measurements. The growing dielectric layer on the anode of the PM shifted the electrical potential of the anode during deposition from ground to negative values, making it more and more difficult for electrons to escape from the plasma. To prevent electrons from going to the stress monitor and influencing the growing film (e. g. heating) the stress monitor had to be isolated from ground. The resulting floating potential of the whole in-situ stress monitor was typically in the range between - 35V and -45V with respect to ground.

The result of this procedure was a decrease in substrate heating to about 330K to 345K. Before the electrical isolation of the stress monitor the temperatures rises during deposition were higher, ranging from 420K to 720K, due to current heating by plasma generated electrons.

The second mean to improve the otherwise poor reproducibility of the stress measurements was a reset of the vacuum chamber's inner walls, anode and target surface by aluminizing them before each AlN deposition and stress measurement.

Further the simplicity of the experimental set-up also contributed to the reproducibility of the measurements. Therefore

no shields were used in these experiments. Operational data are recorded in Table 1.

Table 1. Reactive magnetron-sputtering system parameters used to deposit AlN thin films on different substrates.

Vacuum system:	Oil diffusion pumped residual gas pressure: 2×10^{-4} Pa
Sputtering system:	Planar magnetron cathode pure Al target (99.999%), $12.5 \times 25 \text{ cm}^2$ dc power 1kW discharge voltage 230V - 300V
Sputtering gas:	Argon (99.998%) Nitrogen (99.995%)
Presputtering:	approx. 60seconds
Film thickness:	200nm to 400nm
Substrate temperature:	starting at room temperature. up to 340K
Substrate to target distance:	0.14m
Substrate:	Fused silica for stress measurements, silicon for AES, and amorphous carbon for TEM

3. Results

Published data ³⁻⁹ and our own preliminary measurements¹² enabled the choice of a promising range of variation for the parameters Ar/N₂ ratio and total gas flow. The argon to nitrogen ratios varied from 1:3 to 3:1 at three different total gas flows:

50sccm,
100sccm, and
200sccm.

The following parameters influenced the stress values of the dc magnetron sputtered AlN thin films:

- Plasma parameters,
- substrate temperature,
- deposition rates.

In addition the following features of the thin films were investigated:

- structure and morphology,
- refractive index,
- and optical absorption

3.1 Plasma parameters

By varying the sputtering parameters in the case of a pure Ar discharge (total working gas pressure, discharge power, distance between cathode and substrate, and anode potential) the changes on the magnetron plasma parameters have been investigated.

3.1.1 Kinetic temperature for pure Al sputtering

The kinetic temperature of electrons was determined by a Langmuir probe placed in the positive column of the magnetron discharge in a distance of about 8cm away from the Al cathode surface. A "high energy" electron group with a kinetic temperature of about $2.5 \times 10^4 \text{K}$ and a density of approx. $1 \times 10^{15} \text{m}^{-3}$ to $3 \times 10^{15} \text{m}^{-3}$ and a "low energy" electron group with a kinetic temperature of about $1 \times 10^4 \text{K}$ and a density of approx. $3 \times 10^{15} \text{m}^{-3}$ to $1 \times 10^{16} \text{m}^{-3}$ were experimentally determined. The

measured energy distribution was a superposition of two Maxwellian distribution functions. This is often observed in hollow cathode gas discharges.¹³ A variation of the sputtering gas flow exhibited a significant increase of the "low energy" electron group, whereas the value for the "high energy" electron group remained constant. The resulting density ratios of the two electron groups are displayed in fig. 3.

3.1.2 Plasma-potential and floating-potential for AlN reactive dc magnetron-sputtering

The difference between the plasma-potential and the floating-potential of the glass substrate remained constant even under reactive sputtering conditions when the anode was totally covered with insulating AlN. The obtained value was about -7volts. That means that besides sputtered atoms almost exclusively positive ions and high energetic neutrals were able to reach the substrate surface and could therefore influence both the formation of the film and its stress behaviour.

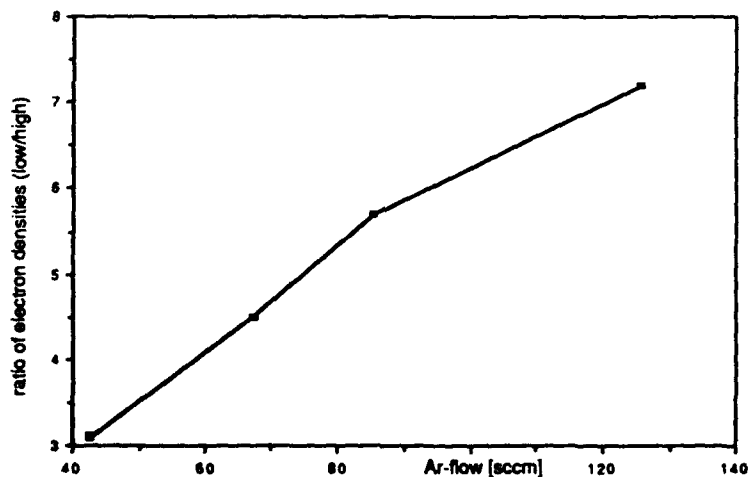


Fig. 3.: Ratios of the measured electron densities for the "low energy" and "high energy" electrons versus the Ar gas flow.

3.2 Thin film parameters

3.2.1 Substrate temperature

Heating effects from particle bombardement can be considerable since a kinetic energy to thermal energy conversion may reach high values for particle energies of few eV. The contribution of fast plasma electrons from the magnetron discharge is regarded to be of minor importance because of the deflecting magnetic field near the cathode surface. Nevertheless, a steady state temperature of the glass substrate of 323K to 343K, was obtained after 5 minutes as can be seen in Fig. 4. (distance: substrate to cathode: 9cm, power: 1kW, gas pressure: 3 to 7x10⁻¹Pa).

Due to deposition rate and plasma parameter measurements three different reasons for substrate heating have to be considered.¹⁴ First, energy from impinging sputtered Al particles of approx. to a maximum value of 24Wm⁻², second, energy from positive ions of approx. to a maximum value of 42Wm⁻², and third, energy from the neutralisation of ions at the substrate of an approximate maximum value of 90Wm⁻².

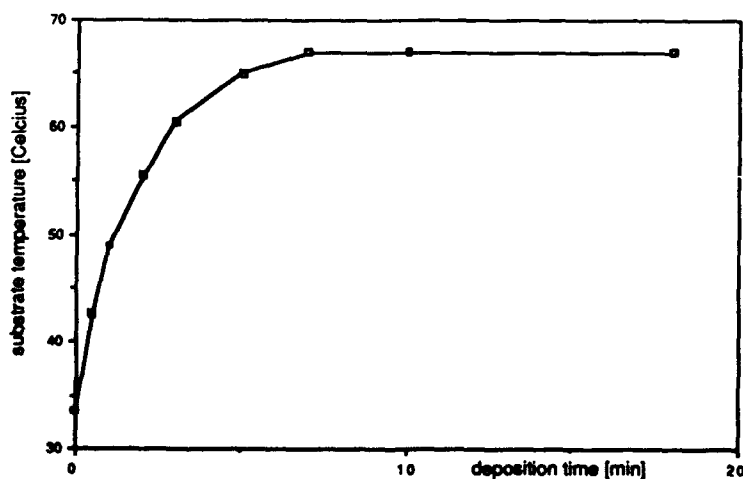


Fig. 4.: Evolution of substrate temperature during reactive sputter deposition (N₂-flow: 75sccm, Ar-flow: 25sccm)

3.2.2 Deposition rates

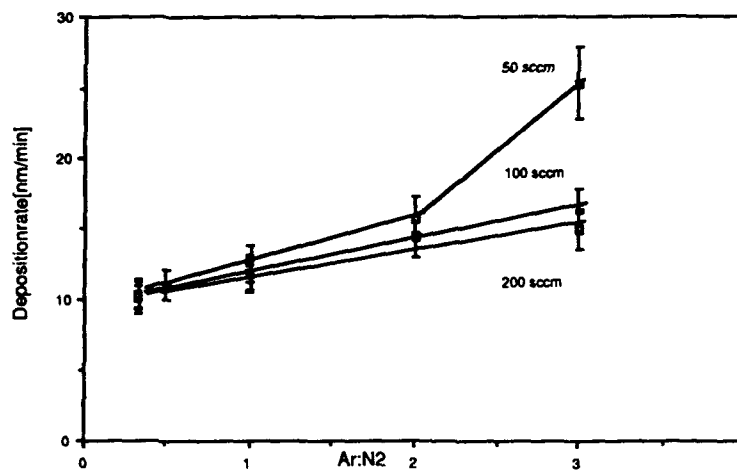


Fig. 5.: Deposition rates of AlN versus gas composition at total gas flows of 50sccm, 100sccm, and 200sccm.

The deposition rate (see fig 5) was found to increase when the total gas flow and the nitrogen fraction in the gas mixture decreased.

The sputtering rate (emitted target mass per time unit) of the target remained unchanged with constant gas-discharge power as long as the sputtered area of the metal surface was clean. An increase of the total gas flow increased the scattering of both sputtered Al and the gas species reflected from the cathode so that less coating material and high energetic neutral gas atoms per time interval arrived at the substrate.

The dependence of the deposition rate on the Ar/N₂ ratio can be explained by the effect of "target poisoning".¹⁵ That is the formation of AlN on the target surface when the partial pressure of the reactive gas exceeds a critical pressure value, that is a function of the sputtering rate of AlN and the standard free energy of formation of AlN. Since the sputtering rate in dc magnetron sputtering is not uniform across the target area, the

"target poisoning" starts at areas of low erosion and spreads over larger target areas with increasing reactive gas pressure. A much lower sputtering yield of that dielectric compound layer is responsible for the rapid decrease in sputtering rate once poisoning has started.

3.2.3 Chemical Composition

The chemical composition of the AlN films was determined by AES depth profiling. The Al to N ratio within the film was found to be close to 1:1 for all AlN samples. Beside Al and N small amounts of O were also detected. A variation of the oxygen content with the deposition parameters was not observed. The oxygen signals of all samples showed higher values at the surface than inside the film. There was no indication of other chemical contaminants.

According to the accuracy of the AES method all films were composed of at least 95% AlN.

All reactively sputtered AlN films had an Al to N ratio of 1:1, even AlN films prepared at high N₂ flows. No excessive nitrogen was detected, which is in agreement with investigations concerning the solubility of nitrogen in AlN films.¹⁶

3.2.4 Morphology and structure

AlN specimens obtained with the extreme values of the sputtering parameter were investigated with TEM. Fig.6 a) to d) shows TEM micrographs taken of AlN films produced in different regimes of gas flow and sputtering gas ratios. In the low-flow regime the crystal size increased from 8nm with a Ar/N₂ ratio of 1:3 (high N₂) to 18nm with a Ar/N₂ ratio of 3:1 (low N₂). In the high-flow regime the observed crystal size of 6nm to 7nm was independent of the Ar/N₂ ratio.

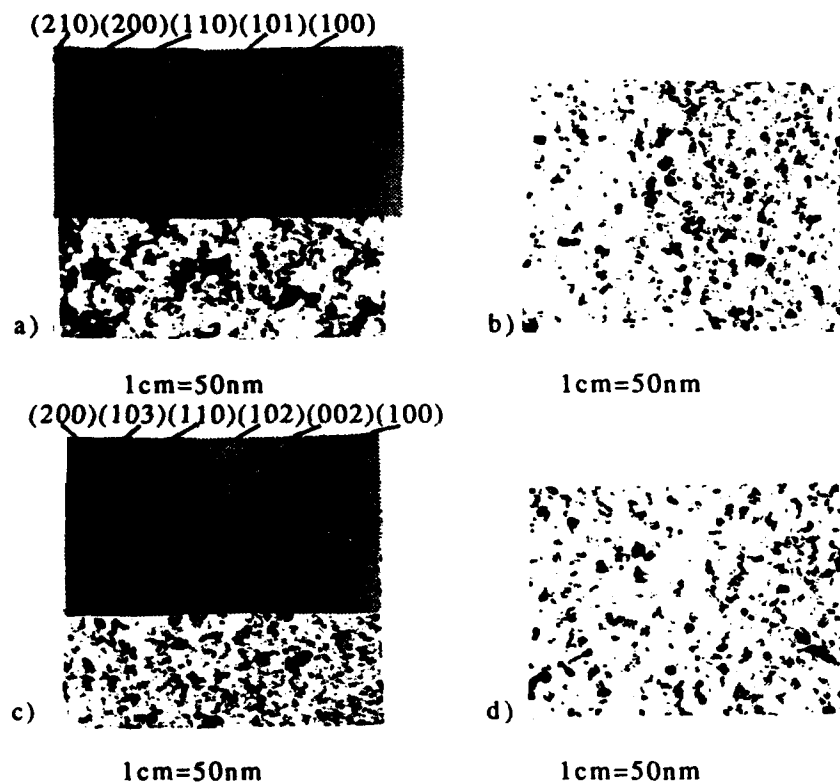


Fig. 6.: TEM micrographs and electron diffractograms (for sputtering gas ratios 3:1 only) of reactively dc magnetron sputtered AlN thin films (magnification 2×10^5) for a) total gas flow of 50sccm, and Ar/N₂ ratio 3:1; b) 50sccm, 1:3; c) 200sccm, 3:1; d) 200sccm, 1:3.

A polycrystalline hexagonal structure of all the AlN films was found by electron beam diffraction. In the case of low sputtering gas pressure of about 2×10^{-1} Pa a preferential orientation with the cristallographic c-axis orthogonal to the substrate was observed. This preferential orientation (texture) vanished as the sputtering gas pressure reached about 8×10^{-1} Pa. This result confirms observations of other authors.^{9,17}

The lattice constants of the investigated AlN-samples were determined from the ring patterns and the TEM-system parameters. The calculated values matched the ASTM-values within the systematic error of 2%.

3.2.5 Optical data

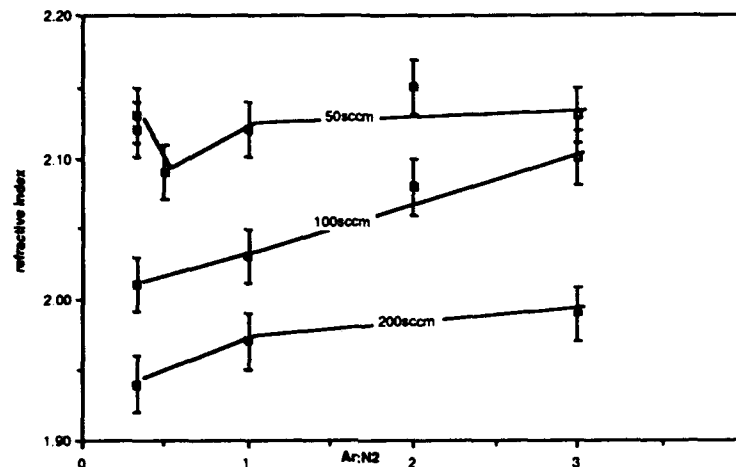


Fig. 7.: Refractive index at 550nm calculated from transmission data of reactively dc magnetron sputtered AlN films of total gas flows of 50sccm, 100sccm, and 200sccm for different sputtering gas ratios (Ar to N₂).

From the transmission data the refractive index of AlN films was calculated. It appeared that the influence of the gas ratio is smaller than the effect due to changing the total gas flow.

The refractive index of the 50sccm series gathered around 2.12, for the 100sccm samples the mean value is 2.05, and for the 200sccm samples a mean refractive index of 1.97 at 550nm was found.

The absorption coefficient α in the visible of all sputter deposited films was in the range of 10^{-4} to 10^{-3} .

In the work of Aita et al.¹⁸ the optical behaviour near the fundamental absorption edge of rf diode sputter-deposited AlN films was investigated. X-ray diffraction of their films showed the films to be of microcrystalline structure. No further data concerning the size of the microcrystallites was supplied.

The shapes of the measured fundamental absorption edges for various AlN film samples were typical for disordered semiconductors. Following the theoretical considerations of Abe and Toyozawa¹⁹ and the application of the theory to amorphous Si by Cody²⁰ the exponential part of the absorption edges is a consequence of weakened interatomic bonds. Distorted bonding angles, stretched bonding lengths or hybridization with antibonding states may cause such weakening.

As a special feature a shoulder appeared in the low energy part of the absorption edges derived by Aita et al.¹⁸ This shoulder is due to transitions between localized electronic states in the gap and the conduction band. The physical effect responsible for the localized gap states are deviations of the coordination number from the number of the fully coordinated crystalline material.²¹

Our measured optical absorption edges for various gas flows at different Ar/N₂ ratios are shown in figs 8 a-c. Similar to rf sputter-deposited AlN films the investigated AlN films that were deposited by dc magnetron sputtering revealed also three regions in the measured absorption edges.

Optical absorption edge of AlN

Ar:N₂=3:1

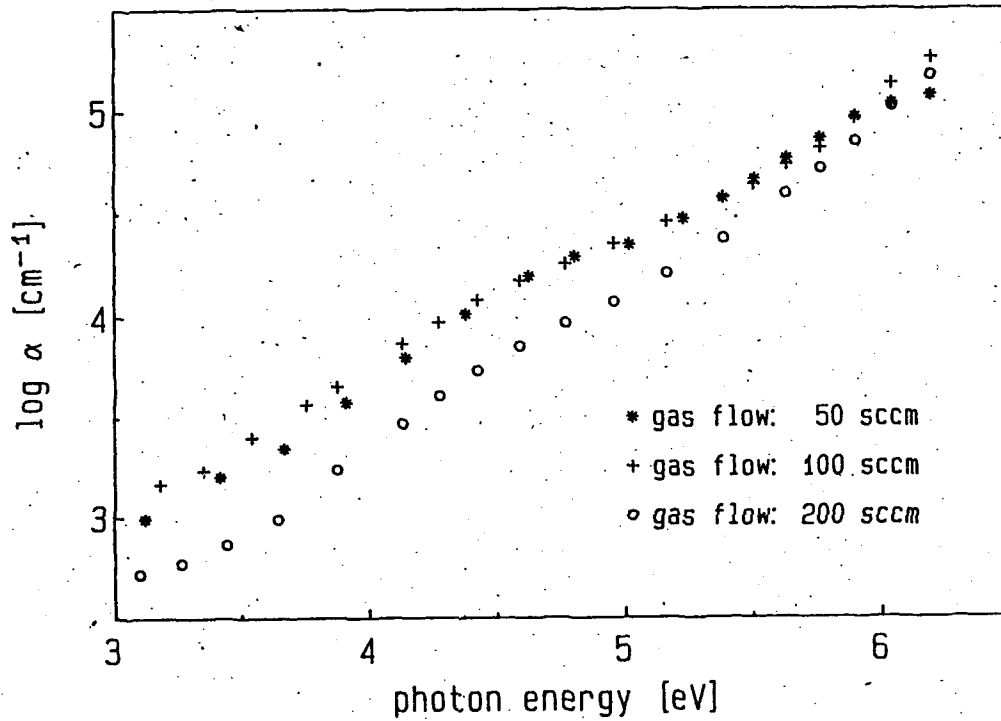


Fig. 8a.: Optical absorption edge of AlN films deposited by reactively dc magnetron sputtering at different total gas flows of 50sccm, 100sccm, and 200sccm for an Ar/N₂ ratio of 3:1.

Optical absorption edge of AlN

Ar:N₂=1:1

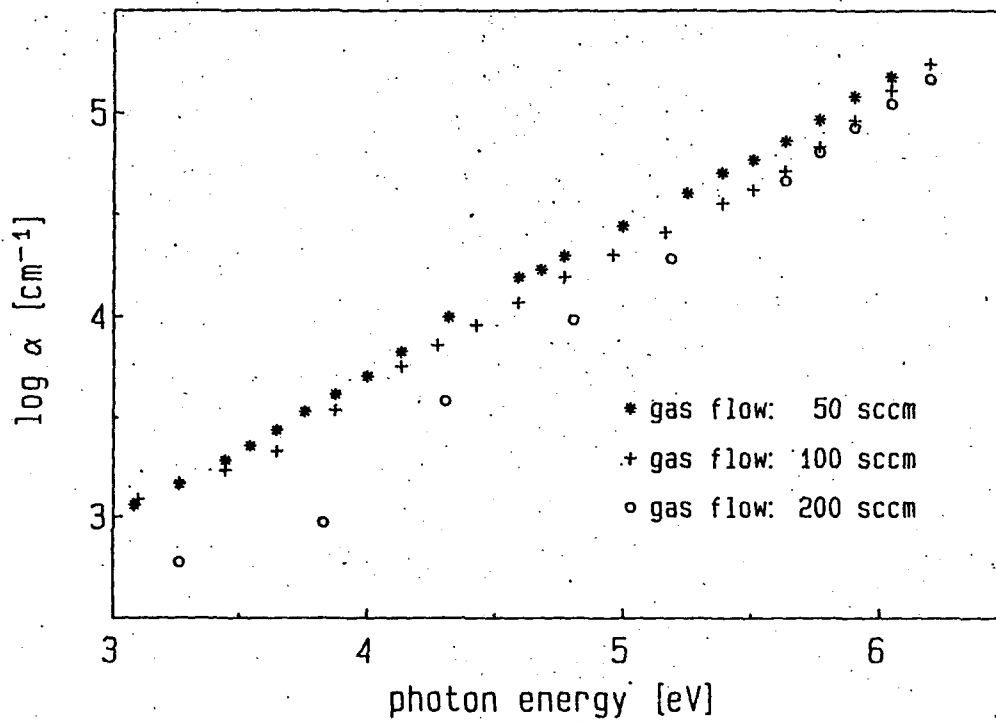


Fig. 8b.: Optical absorption edge of AlN films deposited by reactively dc magnetron sputtering at different total gas flows of 50sccm, 100sccm, and 200sccm for an Ar/N₂ ratio of 1:1.

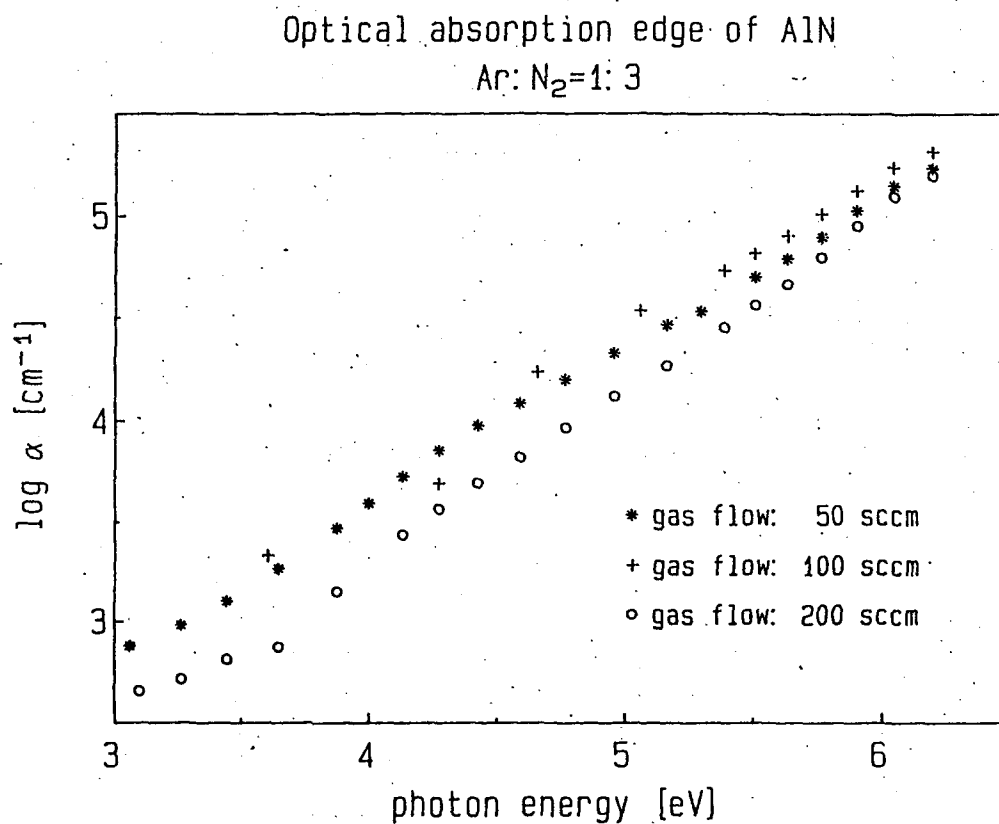


Fig. 8c.: Optical absorption edge of AlN films deposited by reactively dc magnetron sputtering at different total gas flows of 50sccm, 100sccm, and 200sccm for an Ar/N₂ ratio of 1:3.

However, only the films deposited at an Ar/N₂ ratio of 3:1 exhibited a pronounced low energy shoulder. The low energy part of the absorption edges of all other films hardly deviated from a purely exponential shape. The inverse slopes of the curves in the middle energy region are proportional to the degree of disorder of the material.²² AlN film samples prepared at a total gas flow of 200sccm had inverse slope values between 1.01eV to 1.05eV. Films deposited at 100sccm and 50sccm gave inverse slope values from 1.13eV to 1.24eV and from 1.19eV to 1.29eV respectively.

3.3 Stress

3.3.1 Stress tuning

Reactive dc magnetron sputtering of Al in an Ar/N₂ atmosphere was applied for the deposition of AlN thin films. By both, setting the total gas flow at 50sccm, 100sccm, and 200sccm and varying the Ar/N₂ ratio from 3:1 to 1:3 in each gas flow regime, thin AlN films in different states of mechanical stress were obtained.

Figure 9 shows the obtained stress values of the AlN films at different total gas flows and sputtering gas ratios.

The AlN films prepared at gas flows of 100sccm 200sccm showed only tensile stresses (up to 1GPa). The influence of working gas composition was not very pronounced but gave rise to higher tensile stress values for an increasing Ar-fraction.

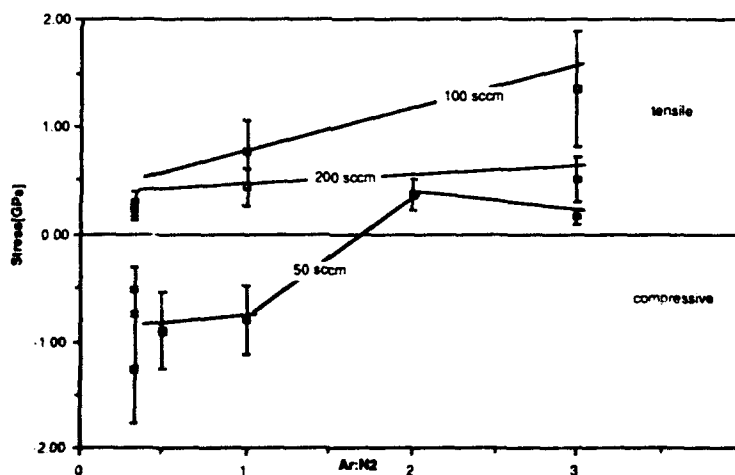


Fig. 9.: Measured stress values of reactively dc magnetron sputtered AlN films for total gas flows of 50sccm, 100sccm, and 200sccm at different sputtering gas compositions (Ar to N₂ ratio).

The 50sccm series showed a transition from compressive (-1.3GPa) to tensile film stresses (0.3GPa) when the Ar/N₂ ratio was increased to more than 2:1. In this flow regime stress tuning was therefore possible.

3.3.2 Reactive Sputtering Model

The reactive sputtering process was described by S. Berg et al.¹⁰ by the following equations:

$$q_0 = q_t + q_c + p_N S, \quad (1)$$

$$0 = 2 F(1 - O_1) - (j/e) S_N O_1, \quad (2)$$

$$0 = 2 F(1 - O_2) + (j/e) S_N O_1 (A_t/A_c)(1 - O_2) - (j/e) S_M (1 - O_1)(A_t/A_c) O_2 \quad (3)$$

$$q_t = F(1 - O_1) A_t, \quad (4)$$

$$q_c = F(1 - O_2) A_c \quad (5)$$

Equation (1) establishes equivalence between the supply of the reactive gas (q_0) and its consumption by the target (q_t), the chamber (q_c), and the pump ($p_N S$). Equation (2) describes the reactive gas balance at the target and Eq. (3) at the substrate and the vacuum chamber wall.

The parameters are described as follows:

- p_N , N₂ partial pressure;
- S , pumping speed;
- γ , sticking coefficient of nitrogen to Al;
- F , flux of N₂ due to p_N [$F = p_N / (2 m k T)^{1/2}$, N₂ molecular weight m , gas temperature T , Boltzmann constant k];
- O_1 , nitride coverage of the target (cathode);
- O_2 , nitride coverage of the chamber wall and the substrate;
- S_N, S_M , sputtering yields of nitride and metal;
- j , discharge current density;
- e , elementary charge;
- A_t, A_c , area of the target and the chamber wall.

In this model discharge current and sputtering yield are assumed to be constant. However, due to the nonlinear change of

N_2 partial pressure and the partial coverage of the cathode with insulating AlN in the hysteresis region the discharge resistance is not constant as it was shown experimentally by McMahon²³. Furthermore it is well known that the sputtering yield is energy dependent. Therefore, premising constant discharge current, the sputtering yield is not constant.

To avoid this inadequacy we allow the sputtering yield to depend linearly on the discharge voltage: $y=aU$. This is in good agreement with experimental data on sputtering yields of several materials sputtered by argon ions in the energy range from about 200 to 300eV²⁴, which is typical for our system. This assumption is also supported by the theoretical considerations treating the energy dependence of the sputtering yield in the energy range from sputtering threshold energy up to a few hundred electron volts.²⁵

With this improvement all terms of the form $(j/e)S_i$ ($i=M,N$) in the original model can be replaced by $[(jU)/e]a_i$ ($i=M, N$; a_i constants). These terms remain constant during the sputtering process since the discharge power is kept at a constant level.

Calculations of p_N versus N_2 flow for different pumping speeds and discharge powers based on this model are plotted in figs. 10 and 11. To check the validity for sputtering of AlN the change of N_2 partial pressure owing to a change in N_2 flow was measured using a differentially pumped quadrupole mass spectrometer. The results for various sputtering parameters are shown in figs. 12 and 13.

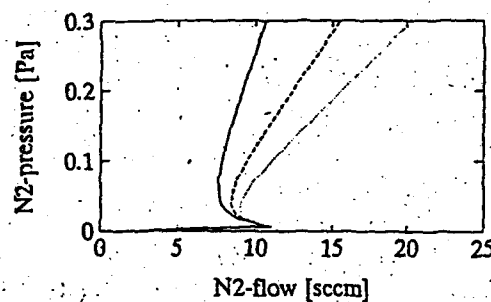


Fig. 10.: Calculated N_2 -partial pressure versus N_2 -mass flow for different pumping speeds:—0.02m³/s---0.04m³/s.....0.06m³/s (discharge power: 2kW, $A_c=0.1\text{m}^2$, $A_l=0.028\text{m}^2$, $a_M=2\times 10^{-3}\text{V}^{-1}$, $a_N=4\times 10^{-4}\text{V}^{-1}$)

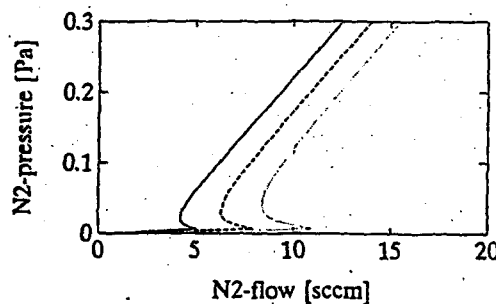


Fig. 11.: Calculated N_2 -partial pressure versus N_2 -mass flow for different power levels:—1.0kW---0.015kW.....2.0kW (pumping speed: 60l/s, $A_c=0.1\text{m}^2$, $A_l=0.028\text{m}^2$, $a_M=2\times 10^{-3}\text{V}^{-1}$, $a_N=4\times 10^{-4}\text{V}^{-1}$).

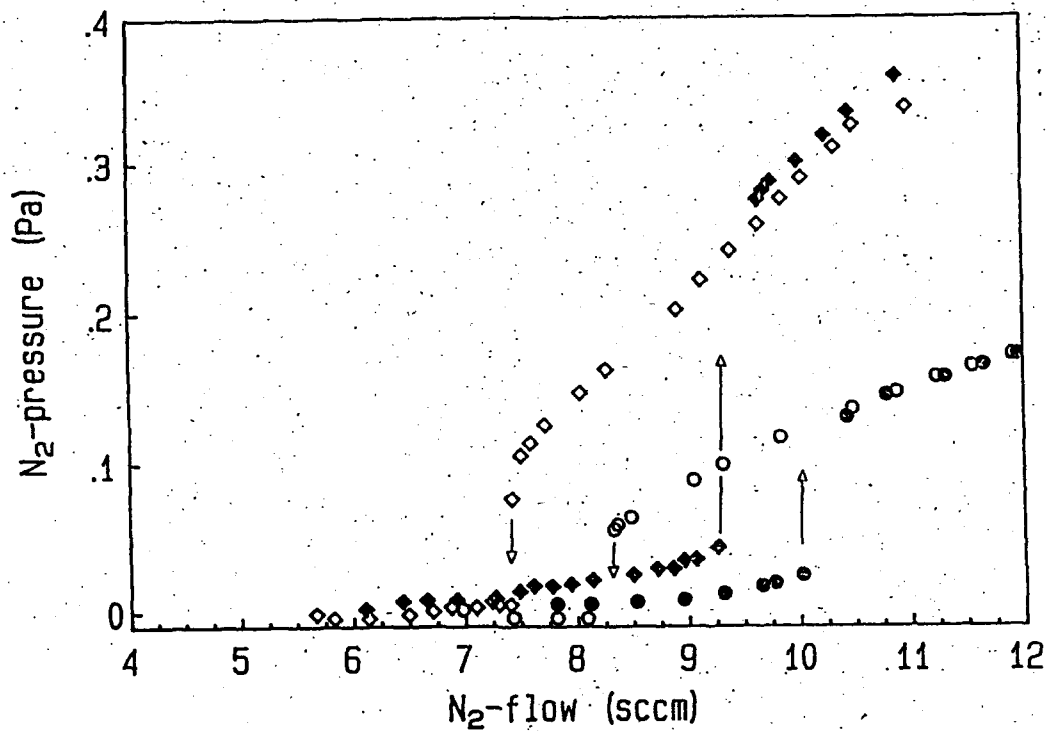


Fig. 12.: Measured N₂-partial pressure versus N₂-mass flow for different pumping speeds: \diamond \blacklozenge 0.02 m³/s, \circ \bullet 0.06 m³/s (discharge power: 2 kW). Filled symbols denote process points reached if starting with a pure Al target (i. e. if starting from the low flow region), unfilled symbols if starting with a partially covered cathode (i. e. if starting from the high flow region).

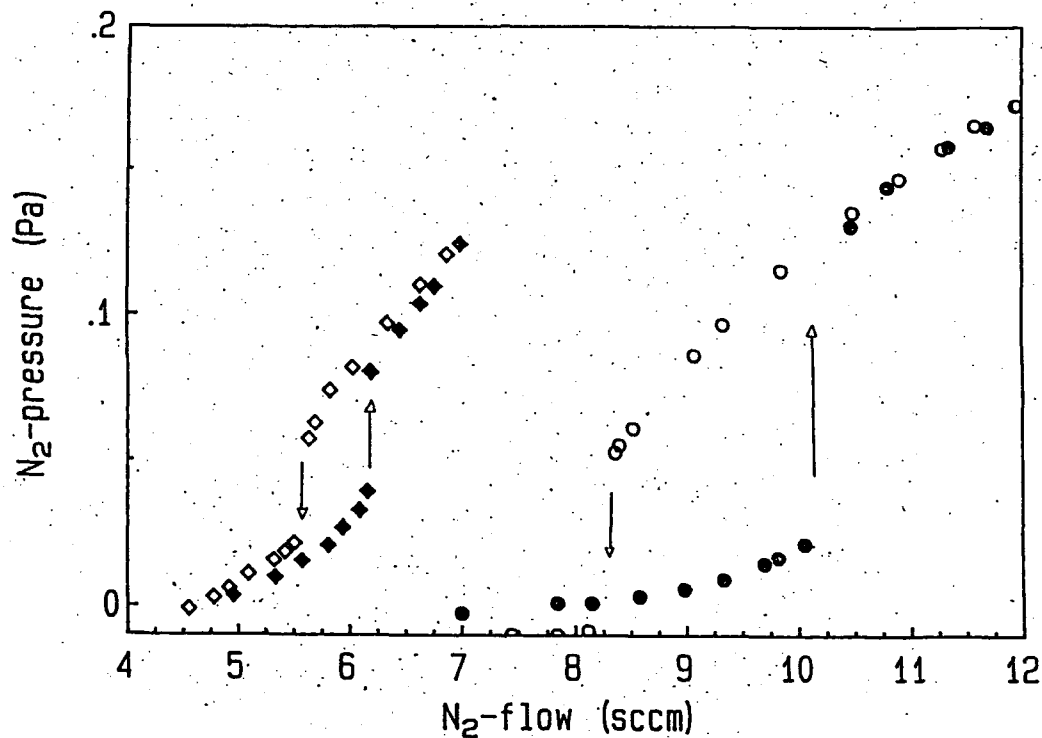


Fig. 13.: Measured N₂-partial pressure versus N₂-mass flow for different discharge power levels (◊ 1kW, ○ 2kW; pumping speed: 60l/s). Filled symbols denote process points reached if strating with a pure Al target (i. e. if starting from the low flow region), unfilled symbols if starting with a partially covered cathode (i. e. if starting from the high flow region).

4. Conclusions

4.1 Deposition parameters

As the discharge power is kept constant, the sputtering rate of target material was also constant, as long as the sputtered surface remained clean of AlN. An increase of total gas flow increased the scattering of both sputtered and reflected particles from the cathode and therefore less particles per second arrived at the substrate.

The distance between target and substrate as well as the total gas pressure (besides other sputtering parameters) determine the kinetic energy of the impinging ad-atoms and the reflected neutrals.

The dependence of the deposition rate on the Ar/N₂ ratio can be explained by the effect of "target poisoning".¹⁵ That is the formation of AlN on the target surface when the partial pressure of the reactive gas exceeds a critical value P_0 , that is a function of the sputtering rate of AlN and the standard free energy of formation of AlN. As the sputtering rate in dc magnetron sputtering is non uniform across the target area, the "target poisoning" starts at places of low erosion and grows with increasing reactive gas pressure. A much lower sputtering yield of the dielectric compound layer on the target is responsible for the rapid decrease in sputtering rate once poisoning has started.

The choice of the process parameters to be varied is decided by the need for a demand of proper stoichiometry, good tuning and easy handling. Usually the gas compositions - (in this context the argon to nitrogen ratio) - and the total gas flow are taken as variable process parameters.

Changes in these two parameters cause modifications of discharge voltage and current, deposition rate, heat transfer to the substrate, etc. It is not surprising that due to these parameter changes the properties of the deposited films tend to vary

remarkably. In the reactive sputtering it is possible to modify chemically the material that is deposited, as the gas composition defines the mode of deposition. Here sputtering in an inert atmosphere with low reactive gas (nitrogen) content is called the metallic mode and produces metallic aluminum films with some nitrogen in it, whereas sputtering in the dielectric mode with sufficient or surplus reactive gas produces AlN coatings. In between the two modes substoichiometric AlN_x films can be obtained. However, as already mentioned above always conditions were chosen for stoichiometric AlN deposition.

4.2 Morphology and structure

The evaluation of TEM photographs provided crystal grain sizes of the obviously polycrystalline AlN films. Regarding the stress values of the 50sccm series, the compressive stresses are aligned with diameters of crystal grains of 8nm and the tensile stresses go along with 18nm diameter. For the 200sccm series two thin films were investigated, namely with Ar/N₂ ratios of 3:1 and 1:3. Both samples showed tensile stress of about 0.4GPa. The measured crystal size of both was 5nm to 6nm.

4.3. Optical absorption

The structural disorder of AlN thin films produced by both rf and dc sputtering procedures is apparent in optical absorption measurements.¹⁸ Actually three energy regions were found where the dependence of the absorption coefficient α on incident photon energy E varied.

- $(E-E_g)^2$ region (above 6.2eV): Near the high energy end of the edge, i.e. close to the bandgap energy E_g , α was found to be proportional to $(E-E_g)^2$. This is the energy region where valence band to conduction band transitions occur. The transition probability is proportional to $(E-E_g)^2$ as a consequence of the same energy dependence of the relevant joint density of states.

- Exponential region ($5.5\text{eV} < E < 6.2\text{eV}$): Decreasing the photon energy E a region of exponential dependence of α on E adjoins. Structural or thermal disorder of the material remove the singularities of the density of states at the band edges and replace them by exponentially decreasing tails stretching themselves into the gap area. Transitions from this tail states to the band states, or vice versa, cause the exponential slope of the absorption edge of disordered materials.

According to Ref 18 the absorption edge of any form of AlN can be fitted to the equation

$$E_x(W,T) = E_g - AE_0(W,T)$$

where A is a material constant, E_x is the energy band gap of the disordered crystal, E_0 is the inverse slope in the region of incident photon energy where the absorption coefficient has an exponential dependence on incident photon energy, E_g is the band gap of the virtual crystal, W is the structural disorder parameter and T is temperature. Values for E_g ($=6.18\text{eV}$) and A ($=2.3$) were taken from the above mentioned reference. Inserting our obtained values of E_0 resulted in E_x ranging from 3.1eV (for the 50sccm samples) to 3.9eV (for the 200sccm samples).

In the exponential region lower inverse slope values E_0 of the 200sccm samples indicated less disorder than the 100sccm and 50sccm samples. This states the influence of the kinetic energy of the condensing film particles.²⁶ Due to gas scattering the loss of kinetic energy is proportional to the total sputtering gas pressure.

- Shoulder region ($4.5\text{eV} < E < 5.5\text{eV}$): At the lower end of the absorption edge α left the exponential dependence on E and a marked shoulder appeared. Deviations in the coordination number of film atoms cause localized electronic states inside the bandgap. Transitions between these localized states and band states give rise to the observed shoulder in the absorption behaviour.

The appearance of the shoulder in the low energy region was restricted to films sputtered with an Ar/N₂ ratio of 3:1. The high

Ar content in the sputtering gas seems favorable for the creation of localized states in the energy gap.

4.4 Thin Film Stress

4.4.1 Model

A model that is widely accepted for explaining the origin of compressive stress in sputter deposited films is the atomic peening model: film structure and stress state depend on the energy of the particles-(coating material or gas)-striking the growing film. The intrinsic tensile stresses in our experiments are mainly caused by the less dens, mostly columnar microstructure of the deposited films. The low film packing density is a consequence of the insufficient mobility of the condensing coating material atoms on the substrate and the film surface respectively. In the case of low pressure sputtering the mobility of these ad-atoms is enhanced by their own kinetic energy, which is initially in the range of 5eV to 20eV, and by bombardment of highly energetic neutral atoms of the working and reactive gas (approx. up to 100eV) that are reflected from the target. The resulting forward sputtering effect caused mainly by the fast neutrals is assumed to densify the film microstructure and to be responsible for compressive stresses in reactively sputter deposited thin films.²⁷

The distance between target and substrate as well as the total gas pressure (besides other sputtering parameters) determine the kinetic energy of the impinging adatoms and the reflected neutrals.

4.4.2 Reactive dc magnetron sputtering

Reactive dc magnetron sputtering of Al in an Ar/N₂ atmosphere was applied for the deposition of AlN thin films. By both setting the total gas flow at 50sccm, 100sccm, and 200sccm and varying the Ar/N₂ ratio from 3:1 to 1:3 in each gas flow thin films in different states of mechanical stress were obtained.

In this study the samples of the series with 100sccm and 200sccm total gas flow, corresponding to working gas pressures of 4×10^{-1} Pa and 8×10^{-1} Pa respectively, resulted in such a strong gas scattering by inelastic collisions of the sputtered target particles as to leave them with only thermal energies (in the range of tens of meV) when they arrived at the substrate. Films with low packing density and the corresponding tensile stresses similar to evaporated films were the result of this thermalization of the sputtered coating material. The reflected neutrals might have also been subject to strong scattering as the occurring tensile stress suggests.

Less gas scattering and therefore higher kinetic energy of the sputtered coating material atoms and of the reflected neutralised nitrogen atoms give rise to compressive stresses or at least minor tensile stresses in the films of the 50sccm series. The compressive stress values increase with increasing nitrogen content in the working gas. This behaviour is known 28, 29 and explained by the increasing coefficient of reflection for particles at the target, with increasing $M_{\text{target}}/M_{\text{ion}}$ mass ratio.

Although the extreme values of the stress in AlN films were - 0.9GPa on the compressive and +1.2GPa on the tensile side, no significant differences in the aluminum to nitrogen ratio could be detected. This result supports the knowledge that predominantly the film microstructure determines the intrinsic stress.

Regarding the stress values of samples of the 50sccm series, the compressive stresses are aligned with densely packed crystals of grain diameters of about 8nm. Tensile stresses are related to lower packed crystals and grain diameters with about 18nm. From the 200sccm series two thin films were investigated, obtained with Ar/N₂ ratios of 3:1 and 1:3. Both less densely packed samples with measured crystal size between 5nm to 6nm showed tensile stress of about 0.4GPa.

Obtained stress values of the AlN films are in agreement with data from other authors [9, 30]

AlN samples with low tensile ($<0.4\text{GPa}$) or compressive stress values yield refractive indices between 2.12 and 2.16. In the regime of tensile stress larger than 0.4GPa the refractive indices ranged from 1.94 to 2.07. The higher refractive index in films with compressive stress values seems to be a consequence of the generally higher density of such thin films.

Klaus L. Füller

Prof. Dr. phil. H. K. Pülker

22. Jan. 1992

E. Rille

DI. Dr. techn. E. Rille

22. Januar 1992

5. References

1. M. D. Thouless, Thin Solid Films 181,397(1989).
2. E. Klokholm, IBM J. Rev. Develop., Vol.31 No5, 585(1987).
3. D. W. Hoffman and J. A. Thornton, Thin Solid Films 40, 355(1977).
4. J. A. Thornton and D. W. Hoffman, J. Vac. Sci. Technol. 14, 164(1977).
5. D. W. Hoffman and J. A. Thornton, Thin Solid Films 45, 387(1977).
6. J. A. Thornton, J. Tabock, and D. W. Hoffman, Thin Solid Films 64, 111(1979).
7. D. W. Hoffman and J. A. Thornton, J. Vac. Sci. Technol. 20, 355(1982).
8. A. Entenberg, V. Lindberg, K. Fletcher, A. Gatesman, and R. S. Horwath, J. Vac. Sci. Technol. 5, 3373(1987).
9. G. L. Huffman, D. E. Fahnlne, R. Messier, and L. J. Pilione, J. Vac. Sci. Technol. A7(3), 2252(1989).
10. S. Berg, H. o Blom, T. Larsson, C. Nender, J. Vac. Sci. Technol. A 5(1987)202
- 11 R. Swanepoel, J. Phys. E: Sci. Instrum. 16(1983)1214.
12. R. Zarwasch, E. Rille, and H. K. Pulker, Proc. SPIE Vol. 1019(1988)123.
13. F. Howorka, M. Pahl, Z. f. Naturforschung 27a(10) (1972)1425.
14. J. A. Thornton, Thin Solid Films 54, 23(1978)
15. R. N. Castellano, Proc. 7th Intern. Vac. Congr. & 3rd Intern. Conf. Solid Surfaces (Vienna 1977),p. 1449.
16. J. M. E. Harper, J. J. Cuomo, and H. T. G. Hentzell, J Appl. Phys. 58(1), 550(1985).
17. G. Este and W. D. Westwood, J. Vac. Sci. Technol. A, Vol.5, No4, 1892(1987).
18. C. R. Aita, C. J. G. Kubiak, and F. Y. H. Shih, J. Appl. Phys. 66(1989)4360.
19. S. Abe and Y. Toyozawa, J. Phys. Soc. Jpn. 50(1981)2185.
20. G. D. Cody, in "Semiconductors and Semimetals", Vol. 21, Part B, Optical Properties, ed. J. I. Pankove (Academic Press, Orlando)(1984)11.

21. D. Adler, in "Physical Properties of Amorphous Materials", ed. D. Adler, Brian B. Schwartz, and Martin C. Steele (Plenum Press, New York and London) (1985)5.
22. H. Fritzsche, in "Physical Properties of Amorphous Materials", ed. D. Adler, Brian B. Schwartz, and Martin C. Steele (Plenum Press, New York and London) (1985)313.
23. R. McMahon, J. Affinito, and R. P. Parsons, J. Vac. Sci. Technol. 20(1982)376.
24. G. K. Wehner and G. S. Anderson, "Handbook of Thin Film Technology", eds. L. J. Maissel, R. Glang (McGraw-Hill, New York, 1970), Chap.3-1.
25. P. Sigmund, Phys Rev. 184(1969)383.
26. J. A. Thornton, J. Vac. Sci. Technol., 11(1974)666.
27. H. Windischmann, J. Appl. Phys. Vol. 62, No 5, 1800(1987).
28. D. W. Hoffman and J. A. Thornton, J. Vac. Sci. Technol. 17, 380(1980).
29. J. A. Thornton and D. W. Hoffman, J. Vac. Sci. Technol. 18, 203(1981).
30. F. S. Ohuchi and P. E. Russel, J. Vac. Sci. Technol. A5(4) (1987).